Materials Today: Proceedings 47 (2021) 5907–5911

Contents lists available at ScienceDirect

Materials Today: Proceedings

journal homepage: www.elsevier.com/locate/matpr

Contact resistance prediction of zirconium joints welded by small scale resistance spot welding using ANN and RSM models

Raheem Al-Sabur [a,*], Mikhail Slobodyan [b], Sanjay Chhalotre [c], Manoj Verma [d]

[a] Department of Mechanical Engineering, University of Basrah, Basra 61001, Iraq
[b] Tomsk Scientific Center SB RAS 10/4 Akademichesky Avenue Tomsk 634055, Russia
[c] Department of Mechanical Engineering, Sagar Institute of Science and Technology, Bhopal, India
[d] Department of Energy & Environmental Engineering, Chhattisgarh Swami Vivekanand Technical University, Bhilai, India

ARTICLE INFO

Article history:
Available online 9 May 2021

Keywords:
Resistance spot welding
Zirconium alloys
Response surface methodology
RSM, artificial neural network

ABSTRACT

The total electrical resistance between electrodes is a major factor in small scale resistance spot welding process uncertainty. The initial resistance between electrodes is depending on the current profile, electrode force and dome radius of hemispherical electrodes. A comparison between the experimental results of the expected resistance between electrodes and the predicted values of using ANN and RSM methods is the main goal of this study. E110 zirconium alloy with a thickness of 0.25 + 0.25 mm and 440 MPa tensile strength is used. An increase in dome radius of hemispherical electrodes reduces mean resistance values for zirconium alloy. The rate of preheating current rise has no appreciable effect on stabilization of resistance between electrodes in all cases. Stepwise current rise significantly reduces dispersion of resistance values for zirconium alloy. However, their dispersion significantly decreases after preheating in comparison with initial values. The empirical model predicted by the response surface methodology (RSM) is compared with the backpropagation algorithm model of artificial neural networks (ANN). On zirconium specimens, the absolute maximum error in RSM technique was 9.92% while 4.43%in ANN. Furthermore, in most cases the absolute maximum error in ANN is lower than RSM.

Selection and peer-review under responsibility of the scientific committee of the Technology Innovation in Mechanical Engineering-2021.

1. Introduction

Spot welding is widely used welding applications in industry where the welding joint properties is functional of quality of contact area. It is found in two welding types; electric resistance spot welding and friction stir spot welding where the first one is considered as fusion welding where the second is solid state type[1,2]. In electric resistance spot welding, the heat dissipation intensive to the environment and electrodes is the main difference between the massive thick-walled workpieces and small-scale ones. In small scale resistance spot welding, there is low thermal inertia which lead to nonuniformly in temperature fields and very high rates of heating and cooling. The workpieces bulk resistance and contact resistance between them, beside the resistance between the workpieces and the electrodes, are representing the total electrical resistance (RBE) values which are considered as uncertainty function of the resistance spot welding that led to critical effects on the properties of small-thickness joints. There are several experimental studies focused on the electrode contact resistance before and after welding process by studying the effect of surface condition, electrode force and current on the static resistance at the electrode to workpieces and the workpiece to workpieces[3,4]. According to the Joule equation, resistance contact variation is dependent on the contact area and the nugget size which is affected by electrode force. Despite wide range research in the contact resistance phenomenon, the welding researchers are still puzzling to understand complexity interference of resistance spot welding parameters[5]. In resistance spot welding, the application of electrodes as contact tip workpiece and joining unit has a considerable action on the wear behavior and contacting[6]. The behavior of connection load-bearing and the wear beside the maximum allowable electrode detailing are the main requirements of

* Corresponding author.
E-mail address: raheem.musawel@uobasrah.edu.iq (R. Al-Sabur).

https://doi.org/10.1016/j.matpr.2021.04.431
2214-7853/
Selection and peer-review under responsibility of the scientific committee of the Technology Innovation in Mechanical Engineering-2021.

the electrode geometry selection[7]. The reduction of depth of penetration is not quite enough in type C electrode geometry due to the prevalence of ring weld formation and welding current increasing[8]. De et al. concluded that the fusion zone size at the faying surface of aluminum in resistance spot welding had not been affected by changing of the contact resistance[9].

concluded that the fusion zone size at the faying surface of aluminum in resistance spot welding had not been affected by changing of the contact resistance[10]. Zirconium Alloys E110 (electrolytic manufacturing) and E110G (sponge zirconium manufacturing) have been tested in several studies[11]. Many studies about the zirconium alloys welding such as resistance spot welding, electron- and laser-beam welding are published[12]. Studies of resistance spot welding on zirconium alloys began in the 1960 s. The corrosion resistance and mechanical properties of pure Zirconium (Zr) and Zircaloy-2 (Zr-2) in resistance spot welding was better when they are used in high pressure and temperature conditions in nuclear reactors when using 75 mm dome shape radius [13]. A good Widmanstätten or martensitic microstructure is existing in resistance spot welding specimens when compared with tungsten inert gas (TIG) ones in the comparison of Zircaloy 4 welded-alloy[14]. Improving the properties of Zircaloy-2 spot welding joints was the main goal of incorporating the Zr76Fe4Ni20 metallic glass. The study showed the influence of this incorporation on the grain size, weld nugget, and the existing martensitic phases in the welding zone[15]. The formation of the weld nuggets of the zirconium elements under heat treatment in spacer grids of nuclear reactors is necessary to understand for the manufacturers of E110 and E635 alloys and their application in welding fields[16]. Recently, good development has been applied in zirconium alloys welding by using a computerized power source to control the welding current in resistance spot welding. In this study, preheating pulse (1 kA, 5 ms) , electrode force of 300 with dome shaped electrode was used to investigate the influence of welding pulse duration on the joints properties and microstructure[17]. A new modification for welding the E100 alloy was fabricated on a special welding facility to study the effect of heat treatment and profile of welding current on mechanical properties and microstructure of weldments was shown by using 16 time–current profiles and preheating pulse (1 kA, 5 ms) [18]. Later, the influence of electrode declination on stability of nugget formation of E110 alloy welded by RSW was shown. The effect of the welded joints on the tensile strength and formatted nugget area was studied using special power source current (1 kA) with preheating pulse ,welding pulse, and post-weld pulse of 3, 5 and 3 ms respectively[19]. Presently, the spacer grid is the major application of the zirconium alloys welded by RSW. A specific study was done about the influence of welding parameters on initial resistance between electrodes during the E110 zirconium alloy welded by small scale resistance spot welding using 4 different preheating pulses. In this study, the effect of pre-heating current profiles, dome sphere radius, and electrode force on initial resistance between electrodes was investigated. Furthermore, the study showed the initial contact stabilization is very critical and cannot be solved by machining the electrode tips or increasing electrode force[20]. Sokolov investigated the theoretical analyses in resistance spot welding and indicated the required governing equations[21]. The bulk resistance is dominating the resulted heat generation in the joints:

$$R = k.\rho.\frac{2.\delta}{S_c} \tag{1}$$

where δ is workpieces thickness, ρ is metal specific electrical resistance, Sc is workpieces cross-sectional area and k is spreading coefficient of current.

2. Response surface methodology (RSM)

RSM is a mathematical and statistical optimization tool introduced by Box and Wilson. In this technique, one or more independent variables can be controlling the output variables[22]

$$Y = \varnothing(x_1, x_2, \cdots .x_k) \pm e_r \tag{2}$$

$$Y = b_o + \sum b_i x_i + \sum b_{ij} x_i + \sum b_{ij} x_i x_j + e \tag{3}$$

where the predicted output response is Y, b0 is a constant, bi, bii and bij are the linear, quadratic, and cross product coefficients, respectively.

In most literatures, the output variables called a response function while the independent variables term is used for the input variables in the response surface methodology. Response Surface Methodology had been extensively utilized in many engineering fields such as in the mechanical, chemical, and manufacturing and later expanded to include new branches such as medical applications.

There are many studies tried to optimize the welding parameters or predict the mechanical properties and microstructure of the weldment during RSW by using Response Surface Methodology (RSM) such as optimizing the welding parameters zinc-coated layer of galvanized TRIP steel where the input variables were selected as welding force, welding time beside to the welding current while the indentation and shear strength were selected as output variables[23]. Furthermore, RSM used for predicting the weld zone development welded by the resistance spot welding (RSW). This approach can improve the welding quality and performance in RSW[24,25].

3. Artificial neural network (ANN)

The first attempt to inspire neural networks computational models from the human brain was introduced by Warren McCulloch and Walter Pitts in 1943. There are billions of neurons which are interconnected to pass information across each other. The ANN is used to find a nonlinear relationship between inputs and outputs variables by using propagation neural networks by one or more layers of neurons which are related by weights and biases. The relationship established is needed for weights and biases values updating by training. Back propagation algorithm is focusing on computing the error of the neuron for every layer and its relation to the objective function by least mean square error (MSE). Several studies indicated that the using of the ANN in control of welding machines is strongly successful in preparing the parameters of the welding processes and corresponding predicted joint quality [26,27]. One of the main advantages of ANN is ability to use in multi-input /multi output applications. Electrode force, welding current, welding time and sheet metal thickness are widely used as input variables in ANN application in welding field while the welding quality and dynamic resistance curve are used as objective output which can also expanded to nugget penetration, nugget diameter, indentation depth ..etc.[28].

Due to this, the goal of the present research is to establish behaviour resistance between the electrode in RSW during the welding the Russian zirconium alloy E110 using ANN and RSM. The need to modify a technique that will allow prediction of the behaviour of electrode bulk resistance in small scale resistance spot welding as a dynamic method is the primary relevance of the work where the contact resistance as a function of time, force, and electrode radius. It is useful to mention that all concerning parameters change at same time anywhere the dynamic welding process.

Table 1
E110 Zirconium Alloy Properties [20]

Parameter	Value
Elastic modulus, E (kg mm^2)	9600
Brinell hardness, HB	1.50×10^9
Current spreading coefficient, k	1.04
Poisson's ratio, μ	0.38
Electrical resistivity, ρ (mΩ m)	439
Microhardness, HV (Pa)	2.50×10^9
Electrical resistivity, ρf (mΩ m)	3.0×10^{-4}
Melting temperature, Tf (°C)	1856
Resistance to plastic deformation, σ* (N mm^2)	260

Table 2
Power Source IPTKM-10 Specifications [20].

Parameter	Value
Current pulse duration (ms)	0–60
Discreteness of current pulse duration (ms)	0.1
Discreteness of current control (A)	125
Pulse current (kA)	0.125–10 kA

4. Experimental work

In this study a zirconium alloy E110 (Zr-1%Nb) was taken of thickness of 0.25 + 0.25 mm with hemispherical electrodes. The properties of zirconium E100 alloy given in (Table 1). An invited power source called IPTKM-10 was used where it was described in[20] and given in Table 2.

Fig. 1 indicated the differences of ATC. Mode 1 and mode 2 (Fig. 1a) for discrete current rise algorithms while stepwise current represented by mode 3 and mode 4 (Fig. 1b). Same integral heat input in is used in all cases. Fig. 2 shows the multifactor test for calculating the major reasonable ATC for RBE stabilizing of preheating current pulses.

In this experiment, bronze (Cu-1%Cr- 0.05%Zr) electrodes with dome shape used. The electrode surfaces were clean and degreased with ethyl alcohol and there are no visible defects or oxidation. Ten times for each combination of input parameters were used to calculate RBE values according to Ohm's law and three-point smoothing method. The calculation of initial RBE values is begun after ~ 0.5 ms to complete the transient processes in the secondary circuit on current of 125 A while the final values of RBE were calculated instantly before current was cut off. (shown in Fig. 1).

5. Results and discussions

During this study, two types of techniques are used: Artificial Neural Network (ANN) and Response surface methodology (RSM). The selective data for RSM shown in table 3. In order to study the ability to predict the behaviour of welding resistance response, Response Surface Methodology (RSM) needs specific data to check them. Central Composite Design (CCD) is used with 4 factors, α = 1, 1 replicate, 80 base runs and 1 base blocks. The resulted

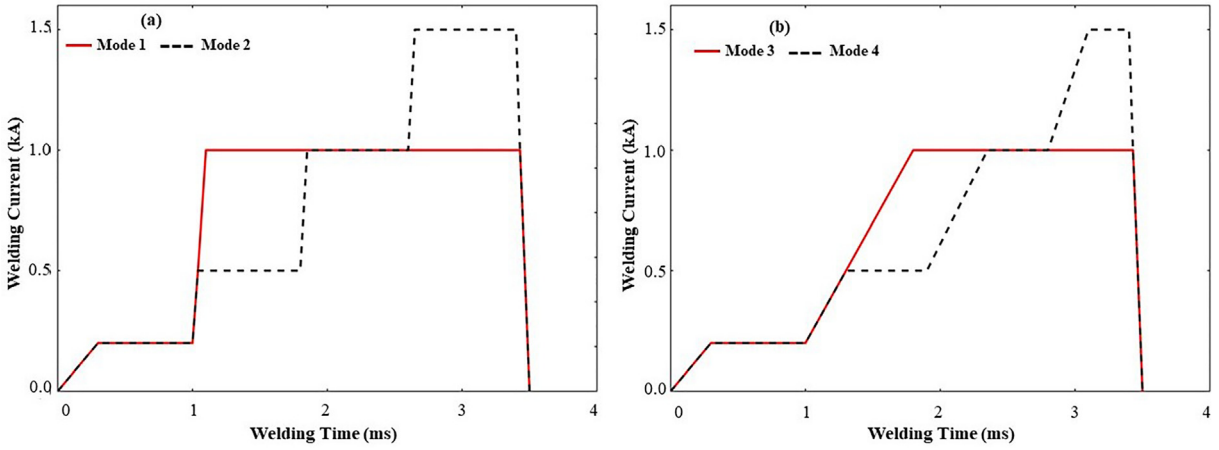

Fig. 1. Current pulses (a) discrete and (b) stepwise.

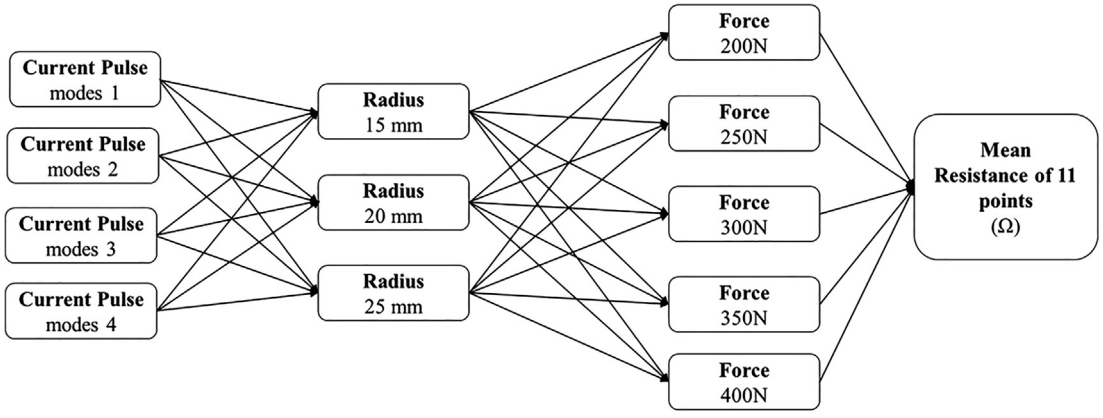

Fig. 2. Scheme of the multifactor experiment.

Analysis of Variance ANOVA shown in table 4 shown that the achieved R-sq is 97.34%, R-sq(adj.) is 96.37% while R-sq(pred.) is 92.44%.

The resulted RSM prediction equations of total electrical resistance between electrodes in Zirconium specimens are depending on the type of current profile as shown below:

Prof	Equation
1	R_Zir = 5.08 + 0.206 r − 0.01085F − 2.213 t − 0.00056 r*r + 0.000012F*F + 0.2854 t*t+ 0.000029 r*F − 0.03820 r*t + 0.000791F*t
2	R_Zir = 6.47 + 0.134 r − 0.01222 F − 2.126 t − 0.00056 r*r + 0.000012 F*F + 0.2854 t*t+ 0.000029 r*F − 0.03820 r*t + 0.000791 F*t
3	R_Zir = 5.20 + 0.203 r − 0.01254 F − 2.073 t − 0.00056 r*r + 0.000012 F*F + 0.2854 t*t+ 0.000029 r*F − 0.03820 r*t + 0.000791 F*t
4	R_Zir = 6.31 + 0.183 r − 0.01214 F − 2.284 t − 0.00056 r*r + 0.000012 F*F + 0.2854 t*t+ 0.000029 r*F − 0.03820 r*t + 0.000791 F*t

The network construction is consisting of four inputs (radius, force, time, profile) and two outputs (resistance of zirconium) with 15 hidden layers. Transfer functions determine a layer's output from its net input where N - S × Q matrix of net input (column) vectors,

Table 3
Response Surface Methodology data.

Run	Radius (mm)	Force (N)	Time (ms)	Prof	Res (Ω)	Run	Radius (mm)	Force (N)	Time (ms)	Prof	Res (Ω)
1	15	200	1	1	4.38	41	15	200	1	3	3.68
2	25	200	1	1	5.20	42	25	200	1	3	5.94
3	15	400	1	1	2.89	43	15	400	1	3	2.95
4	25	400	1	1	6.18	44	25	400	1	3	4.69
5	15	200	5	1	0.51	45	15	200	5	3	0.75
6	25	200	5	1	0.51	46	25	200	5	3	0.67
7	15	400	5	1	0.49	47	15	400	5	3	0.66
8	25	400	5	1	0.52	48	25	400	5	3	0.57
9	15	300	3	1	1.33	49	15	300	3	3	1.35
10	25	300	3	1	1.08	50	25	300	3	3	1.25
11	20	200	3	1	1.49	51	20	200	3	3	1.54
12	20	400	3	1	1.39	52	20	400	3	3	1.39
13	20	300	1	1	4.47	53	20	300	1	3	3.83
14	20	300	5	1	0.54	54	20	300	5	3	0.72
15	20	300	3	1	1.39	55	20	300	3	3	1.44
16	20	300	3	1	1.39	56	20	300	3	3	1.44
17	20	300	3	1	1.39	57	20	300	3	3	1.44
18	20	300	3	1	1.39	58	20	300	3	3	1.44
19	20	300	3	1	1.39	59	20	300	3	3	1.44
20	20	300	3	1	1.39	60	20	300	3	3	1.44
21	15	200	1	2	4.48	61	15	200	1	4	4.49
22	25	200	1	2	4.96	62	25	200	1	4	6.61
23	15	400	1	2	3.83	63	15	400	1	4	4.35
24	25	400	1	2	3.96	64	25	400	1	4	5.19
25	15	200	5	2	0.59	65	15	200	5	4	0.76
26	25	200	5	2	0.48	66	25	200	5	4	0.60
27	15	400	5	2	0.48	67	15	400	5	4	0.59
28	25	400	5	2	0.36	68	25	400	5	4	0.56
29	15	300	3	2	1.15	69	15	300	3	4	1.39
30	25	300	3	2	1.05	70	25	300	3	4	1.37
31	20	200	3	2	1.23	71	20	200	3	4	1.51
32	20	400	3	2	1.13	72	20	400	3	4	1.37
33	20	300	1	2	4.01	73	20	300	1	4	4.48
34	20	300	5	2	0.51	74	20	300	5	4	0.64
35	20	300	3	2	1.17	75	20	300	3	4	1.47
36	20	300	3	2	1.17	76	20	300	3	4	1.47
37	20	300	3	2	1.17	77	20	300	3	4	1.47
38	20	300	3	2	1.17	78	20	300	3	4	1.47
39	20	300	3	2	1.17	79	20	300	3	4	1.47
40	20	300	3	2	1.17	80	20	300	3	4	1.47

Table 4
Analysis of Variance ANOVA.

Source	DF	Adj. SS	Adj. MS	F Value	P Value
Model	21	198.523	9.453	100.93	0.000
Linear	6	161.744	26.957	287.82	0.000
r	1	2.834	2.834	30.26	0.000
F	1	1.169	1.169	12.48	0.001
t	1	156.324	156.324	1669.05	0.000
Prof	3	1.417	0.472	5.04	0.004
Square	3	29.259	9.753	104.13	0.000
r*r	1	0.002	0.002	0.02	0.880
F*F	1	0.162	0.162	1.73	0.194
t*t	1	14.333	14.333	153.03	0.000
2-Way Interaction	12	7.520	0.627	6.69	0.000
r*F	1	0.007	0.007	0.07	0.793
r*t	1	4.668	4.668	49.84	0.000
F*t	1	0.801	0.801	8.55	0.005

Table 5
Comparison between RSM and ANN results.

Parameters				Zirconium Specimens				
Radius	Force	Time	Profile	Exp	RSM	ANN	RSMerror%	ANNerror%
15	300	2	1	4.98	5.31	4.98	6.66	0.13
15	250	5	4	2.61	2.61	2.61	0.15	0.02
15	250	1	3	5.79	5.54	5.77	4.33	0.40
20	200	1	4	4.39	4.68	4.32	6.74	1.60
20	400	2	1	2.69	2.58	2.68	3.96	0.18
20	350	1	4	0.65	0.59	0.66	8.84	1.13
20	250	5	3	0.68	0.70	0.71	4.44	5.08
20	250	3	1	0.69	0.73	0.66	6.57	4.43
20	250	2	2	3.79	3.68	3.73	2.96	1.74
20	400	5	4	1.42	1.39	1.39	2.49	2.47
20	250	1	3	2.50	2.52	2.51	0.87	0.37
25	300	1	2	0.60	0.55	0.61	8.66	1.79
25	250	5	3	4.25	4.44	4.30	4.56	1.14
25	250	2	1	2.97	3.27	2.97	9.92	0.25
25	300	4	1	0.80	0.77	0.82	4.10	2.83

TANSIG (N) takes one input, and returns each element of N squashed between −1 and 1. The number of iterations used is 500 epochs with training error of 1e-7, the above 80 data sets are divided into 40 sets (even) for training and 40 sets (off) for testing.

In order to comparison between the two methods (RSM & ANN), the same data which used in RSM are used again in ANN. The 15 selective below results are taken to achieve the wide range of input parameters.

The data of RSM was achieved using above resulted prediction equations while the results of ANN used directly and shown in table 5. On zirconium specimens, the absolute maximum error in RSM technique was 9.92% while 4.43% in ANN. Furthermore, the most cases the absolute maximum error in ANN lower than RSM. Regarding to the RSM, the best prediction behaviour occurred at radius of 15 mm, force of 250 N, time of 5 ms and profile 4 (stepwise, mode 4) with max error of 0.15% while for ANN is best behaviour occurred with 0.02% at same process parameters.

6. Conclusions

In this study, an attempt to predict the small- scale resistance spot welding total electrical resistance between electrodes using back propagation ANN algorithm and CCD response surface methodology. Both the ANN model and RSM model gave a suitable agreement with the experimental results. The ANN model is a better R2 value (0.98). Regarding the RSM, the best prediction behaviour occurred at radius of 15 mm, force of 250 N, time of 5 ms and profile 4 (stepwise, mode 4) with max error of 0.15% while for ANN is best behaviour occurred with 0.02% at same process

parameters. The maximum error in all tested data was 9.92% in RSM and 4.43% in ANN.

Declaration of Competing Interest

The authors declare that they have no known competing financial interests or personal relationships that could have appeared to influence the work reported in this paper.

References

[1] R.K. Al-Sabur, A.K. Jassim. Friction stir spot welding applied to weld dissimilar metals of AA1100 Al-alloy and C11000 copper. in IOP Conference Series: Materials Science and Engineering. 2018. IOP Publishing. 10.1088/1757-899X/455/1/012087

[2] R. Al-Sabur, A.K. Jassim, E. Messele, Real-time monitoring applied to optimize friction stir spot welding joint for AA1230 Al-alloys, Mater. Today:. Proc. 42 (2021) 2018–2024, https://doi.org/10.1016/j.matpr.2020.12.253.

[3] W. Savage, E. Nippes, F. Wassell, Static contact resistance of series spot welds, Welding J. 56 (11) (1977) 365s–370s.

[4] W.F. Savage, E. Nippes, F. Wassell, Dynamic contact resistance of series spot welds, Welding J. 57 (2) (1978) 43s–50s.

[5] M. Hamedi, M. Atashparva, A review of electrical contact resistance modeling in resistance spot welding, Weld. World 61 (2) (2017) 269–290, https://doi.org/10.1007/s40194-016-0419-4.

[6] M. Tuchtfeld, S. Heilmann, U. Füssel, S. Jüttner, Comparing the effect of electrode geometry on resistance spot welding of aluminum alloys between experimental results and numerical simulation, Weld. World 63 (2) (2019) 527–540, https://doi.org/10.1007/s40194-018-00683-z.

[7] Hicken, S., Metallkundliche Untersuchungen zu Verschleißvorgängen an Elektroden beim Widerstandspunktschweißen von Aluminium. 1997: Shaker.

[8] D. Browne, C. Newton, B. Keay, Aluminum and steel resistance spot welding: Modelling the differences. Advanced Technologies & Processes, IBEC'96, 1996: p. 50-57.

[9] A. De, M.P. Thaddeus, L. Dorn, Numerical modelling of resistance spot welding of aluminium alloy, ISIJ Int. 43 (2) (2003) 238–244, https://doi.org/10.2355/isijinternational.43.238.

[10] Shebaldov, P., et al. E110 alloy cladding tube properties and their interrelation with alloy structure-phase condition and impurity content. in Zirconium in the Nuclear Industry: Twelfth International Symposium. 2000. ASTM International. 1520/STP14316S

[11] S.A. Nikulin, A.B. Rozhnov, V.A. Belov, E.V. Li, V.S. Glazkina, Influence of chemical composition of zirconium alloy E110 on embrittlement under LOCA conditions–Part 1: Oxidation kinetics and macrocharacteristics of structure and fracture, J. Nucl. Mater. 418 (1-3) (2011) 1–7, https://doi.org/10.1016/j.jnucmat.2011.07.017.

[12] M. Slobodyan, Resistance, electron-and laser-beam welding of zirconium alloys for nuclear applications: a review, Nucl. Eng. Technol. 53 (4) (2021) 1049–1078, https://doi.org/10.1016/j.net.2020.10.005.

[13] H. Suzuki, Spot Welding of Zircaloy-2 Alloy Sheets, J. Japan Weld. Soc. 30 (1961) 425.

[14] R. Bordoni, A. Olmedo, Microstructure in the weld region in seam welded and resistance welded Zircaloy 4 tubing, J. Mater. Sci. 16 (6) (1981) 1527–1532, https://doi.org/10.1007/BF00553965.

[15] S. Mishra, R.T. Savalia, K. Bhanumurthy, G.K. Dey, S. Banerjee, Characterisation of metallic glass incorporated Zircaloy-2 weldments, J. Nucl. Mater. 227 (1-2) (1995) 122–129, https://doi.org/10.1016/0022-3115(95)00105-0.

[16] E.V. Yudina, T.M. Poletika, S.F. Gnyusov, L.B. Zuev, Examination of the structural condition of welded joints in zirconium elements of nuclear reactors, Weld. Int. 20 (12) (2006) 965–969, https://doi.org/10.1533/wint.2006.3708.

[17] S.F. Gnyusov, A.S. Kiselev, M.S. Slobodyan, B.F. Sovetchenko, M.M. Nekhoda, A. V. Srukov, P.M. Yurin, Formation of a joint in resistance spot microwelding, Weld. Int. 19 (9) (2005) 737–741, https://doi.org/10.1533/wint.2005.3510.

[18] M.S. Slobodyan, A.S. Kiselev. Optimization of welding parameters for small-scale resistance spot welding of zirconium alloys. in Materials Science Forum. 2019. Trans Tech Publ. 10.4028/www.scientific.net/MSF.970.145

[19] A.S. Kiselev, M.S. Slobodyan. Effects of electrode degradation on properties of small-scale resistance spot welded joints of E110 alloy. in Materials Science Forum. 2019. Trans Tech Publ. 10.4028/www.scientific.net/MSF.970.227

[20] E.Z. Akbolatov, A.S. Kiselev, M.S. Slobodyan, Prediction and stabilization of initial resistance between electrodes for small-scale resistance spot welding, Weld. World 63 (2) (2019) 443–457, https://doi.org/10.1007/s40194-018-0671-x.

[21] N. Sokolov, Microwelding in mass production of radio valve, Publishing house Privolzhsky, Saratov (In Russian), 1971.

[22] R. Al-Sabur, Tensile strength prediction of aluminium alloys welded by FSW using response surface methodology–Comparative review, Mater. Today:. Proc. (2021), https://doi.org/10.1016/j.matpr.2020.12.1001.

[23] Kim, T., H. Park, and S. Rhee*, Optimization of welding parameters for resistance spot welding of TRIP steel with response surface methodology. Int. J. Product. Res., 2005. 43(21): p. 4643-4657. 10.1080/00207540500137365

[24] Muhammad, N., et al., A quality improvement approach for resistance spot welding using multi-objective Taguchi method and response surface methodology. Int. J. Adv. Sci. Eng. Inf. Technol, 2012. 2(3): p. 17-22. 10.18517/ijaseit.2.3.189

[25] N. Muhammad, et al., Optimization and modeling of spot welding parameters with simultaneous multiple response consideration using multi-objective Taguchi method and RSM. J. Mechan. Sci. Technol., 2012. 26(8): p. 2365-2370. 10.1007/s12206-012-0618-x

[26] Thongchai Arunchai, Kawin Sonthipermpoon, Phisut Apichayakul, Kreangsak Tamee, Resistance spot welding optimization based on artificial neural network, Int. J. Manufact. Eng. 2014 (2014) 1–6, https://doi.org/10.1155/2014/154784.

[27] A. El Ouafi, R. Bélanger, J. Méthot, Artificial neural network-based resistance spot welding quality assessment system, Revue de Métallurgie 108 (6) (2011) 343–355, https://doi.org/10.1051/metal/2011066.

[28] A. El Ouafi, R. Bélanger, and J.-F. Méthot. An on-line ANN-based approach for quality estimation in resistance spot welding. in Advanced Materials Research. 2010. Trans Tech Publ. 10.4028/www.scientific.net/AMR.112.141